

Compact Wideband Circularly Polarized SRR Loaded Slot Antenna for Soil Moisture Sensor Application

Puneeth Kumar T. R., Karthik R., Krishnamoorthy K.

Abstract – This paper presents a coplanar waveguide (CPW) fed corner truncated square slot antenna loaded with a split ring resonator (SRR) for soil moisture sensor application. The truncated corner square slot produces a circularly polarized wave with two orthogonal degenerate modes at 4.12 GHz with 3-dB axial ratio bandwidth of 17.69%. Further, the axial ratio bandwidth is increased to 21.81% by loading a rotated SRR on the slot. The split gap of the inner ring of SRR is rotated 90° with respect to outer ring gives circular polarization (CP) at 4.62 GHz. The wideband CP performance is achieved by the combination of truncated corner slot and rotated SRR mode resonances. Both bands are tuned independently to optimize the wide axial ratio bandwidth. The designed antenna is fabricated, and its performance is verified experimentally. The measured impedance bandwidth of 2.53 GHz (61.40%) and axial ratio bandwidth of 0.9 GHz (21.68%) with a peak gain of 2.74 dB is observed. The proposed wideband CP antenna is utilized for soil moisture sensing application and high sensitive microwave sensing application.

Keywords – Wideband, Axial ratio, Circular polarization, Split ring resonator, Soil sensing.

I. INTRODUCTION

The demands of circularly polarized (CP) antennas are increasing nowadays because of their potential to alleviate problems like interference, multipath fading and immune to polarization rotation effect of the electromagnetic (EM) waves [1]. Circularly polarized slot antennas are preferred in modern electronic applications because of their lightweight, easy fabrication and low profile and feeding technique. Metamaterial inspired slot antennas are nowadays becoming popular because of their properties to control EM waves. Researchers are designing split ring resonator (SRR) based slot antennas which are useful in multiband and wideband wireless applications.

Many conventional methods are used to achieve wideband CP performance like stub loaded slot and monopole antennas [2-6]. It is often difficult to design with stub loading method because stubs are much sensitive to design parameters. Single layer broadband CP antennas are designed in [7, 8], but the feeding mechanisms are complex to fabricate. To rectify the

Article history: Received January 08, 2019; Accepted December 23, 2020.

¹Puneeth Kumar T. R. and ¹Karthik R are the Research scholars of Electronics and Communication Engineering, NITK, Suarthkal, Karnataka, India, E-mails: Puneeth.tc@gmail.com and karthik.r.muni@gmail.com

¹Krishnamoorthy K. is the Faculty of Electronics and Communication Engineering, NITK, Suarthkal, Karnataka, India, E-mail: krishnk_ece@yahoo.com

problem of stub loading and complex feeding mechanism, slot-patch combination [9] and SRR based slot antennas are designed. In this design, the bands can tune independently and easy to achieve optimized performance. A dual polarized antenna based on SRR is designed in [10]. A dipole antenna loaded with SRR [11] achieves wideband CP performance, but a complex feeding mechanism is to be used for the dipole. SRRs with a fractal based design [12] and a dual band dual sense circularly polarized truncated square slot antenna is proposed in [13]. In [13], the axial ratio bandwidth is less in both the bands. Also, the truncated square slot alone is not achieving CP. The loading of a pair of SRR achieves CP in both the bands. In the proposed design, the truncated square slot antenna alone achieves wideband CP.

Nowadays the microstrip antennas are becoming potential devices in microwave sensing applications to sense the moisture content of the soil. In [14], a microstrip antenna is used to sense the moisture content by a non-invasive resonance method. An embedded microstrip antenna [15] is used simultaneously for soil sensing and communication to the receiver. Genetic algorithm and the FDTD method is used to sense the soil. A buried microstrip antenna is used to sense the moisture content in the soil [16] by estimating backscatter power. It is a known fact that a narrow-band linearly polarized (LP) antennas often difficult to use for soil-sensing application because they suffer from faraday's rotation due to the variation of moisture content present in the soil. A dual-band CP dielectric resonator antenna (DRA) is proposed for microwave sensing applications [17]. Recently the wideband circularly polarization is achieved using novel feeding network [18] and using multiple modes [19]. These designs have feeding complexity and AR bandwidth is less and cannot be operated over a wide bandwidth. Here, the proposed antenna design provides wideband CP operation, which eliminates the faraday's rotation effect caused by the soil moisture.

In this paper, a novel design of single layer wideband CP truncated square slot antenna loaded with a rotated SRR is proposed to sense the soil moisture. Two orthogonal degenerate modes produced by truncated square slot antenna achieve wideband CP. To further improve axial ratio, an inner ring rotated SRR is designed in the slot. Both SRR and slot resonances are tuned independently to optimize the axial ratio and impedance bandwidth. A simple CPW feed is used to excite the slot antenna. The proposed antenna is used for soil moisture sensing application by investigating change in the reflection coefficient of dry and wet soil. In practical scenario, the wet and dry soil has different dielectric constant. The dielectric constant of wet and dry soil is imitated in the simulator to observe the variation of reflection coefficient.

II. PROPOSED ANTENNA GEOMETRY

The geometry of the proposed SRR loaded slot antenna for CP application is shown in Fig. 1. It consists of a slot antenna and SRR. The proposed antenna is designed using Rogers R04003C substrate with $\epsilon_r = 3.38$, thickness $h = 1.52$ mm and $\tan\delta = 0.0027$. The slot antenna is excited by a 50Ω CPW feed line. The slot antenna and SRR are etched on top of the substrate. The resonance frequency [14] of the slot antenna is determined by,

$$f = \frac{c}{2S_l} \sqrt{\frac{2}{\epsilon_r + 1}} \quad (1)$$

where, c is the speed of light in air and $S_l = (a + s)$ is the length of the square slot. The SRR has radii of R_1 and R_2 forming an outer and inner ring with a strip width of w . The spacing between rings is d and identical split gaps in both rings are $g_1=g_2=g$.

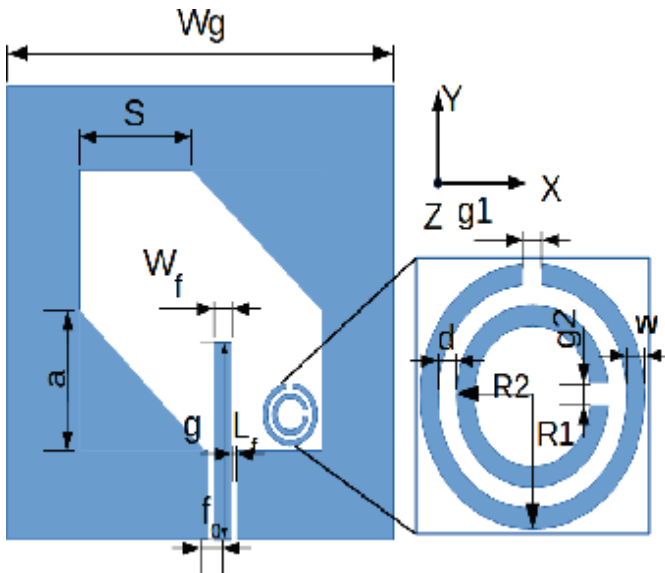


Fig. 1. Top view of the proposed antenna: $W_g=70$ mm, $S=26$ mm, $a=8.4$ mm, $W_f=3$ mm, $g=0.3$ mm, $f_0=3$ mm, $L_f=33$ mm

The designed rotated SRR resonates at 4.62 GHz with parameters given by $R_1=2.8$ mm, $R_2=2.1$ mm, $w_1=w_2=0.5$ mm, $d=0.2$ mm, $g_1=g_2=0.4$ mm. Eq. (2) gives the resonance frequency [20] of the rotated SRR.

$$f_0 = \frac{1}{2\pi \sqrt{\frac{(L_T(\pi+q)^2*\theta^2}{2(\pi+q)} r_{avg} C_{pul}}} \quad (2)$$

where, $= \frac{C_g}{r_{avg} C_{pul}}$, C_{g1} and C_{g2} are the split gap capacitances of two rings, r_{avg} is uniform average dimension of inner and outer ring of SRR, C_{pul} is capacitance per unit length between the inner and outer rings of SRR, θ is the angle of rotation of inner ring with respect to outer ring and L_T is the total equivalent inductance for circular rings with circumference $l=2\pi r_0-g$ having thickness $w_1=w_2=w$ is given by

$$L_T = 0.0002 l (2.303 \log_{10} \frac{4l}{w} * 2.451) \quad (3)$$

The capacitances C_1 and C_2 are equal when two split gaps of SRR are aligned in the same axis. When the inner ring is rotated 90° with respect to the outer ring, the values of C_1 and C_2 become unequal. C_1 and C_2 are calculated as $C_1 = (\pi - \theta)r_{avg} C_{pul}$, and $C_2 = (\pi + \theta)r_{avg} C_{pul}$.

III. OPERATING PRINCIPLE

The corner truncation for CP wave in microstrip patch antennas is common in the literature [21]. The proposed work presents cornertruncated slot antenna with a simple microstrip line feed for wideband CP radiation. The reflection coefficient and axial ratio variation with different truncation depth are shown in Fig. 2. The optimum value of parameter ‘a’ is set as 8.4 mm to get the minimum axial ratio of the slot antenna. To improve the axial ratio bandwidth, a rotated SRR is placed on the slot antenna. The equivalent circuit for rotated SRR loaded slot antenna is shown in Fig. 3, where R_s and G_s are the losses in the feed and substrate. L_s is the feed inductance and C_s is the feed gap capacitance.

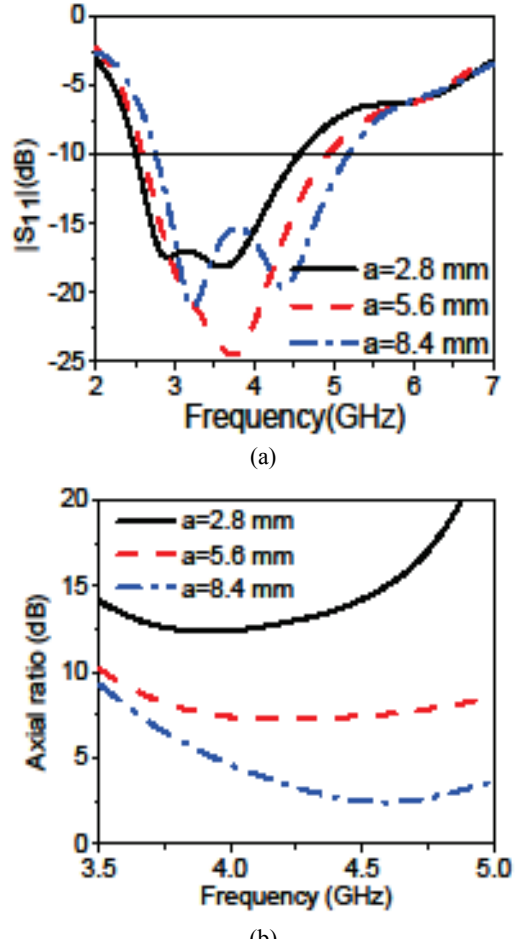


Fig. 2. Simulated reflection coefficient and axial ratio of slot antenna with different values of truncation: (a) S_{11} and (b) axial ratio

L_{sh} and C_{sh} represent the slot. The simplified equivalent circuit of the rotated SRR loaded slot antenna is shown in Fig. 3(b). L_e and C_e are the effective equivalent inductance and capacitance of the rotated SRR. M is the mutual coupling coefficient between the slot and rotated SRR.

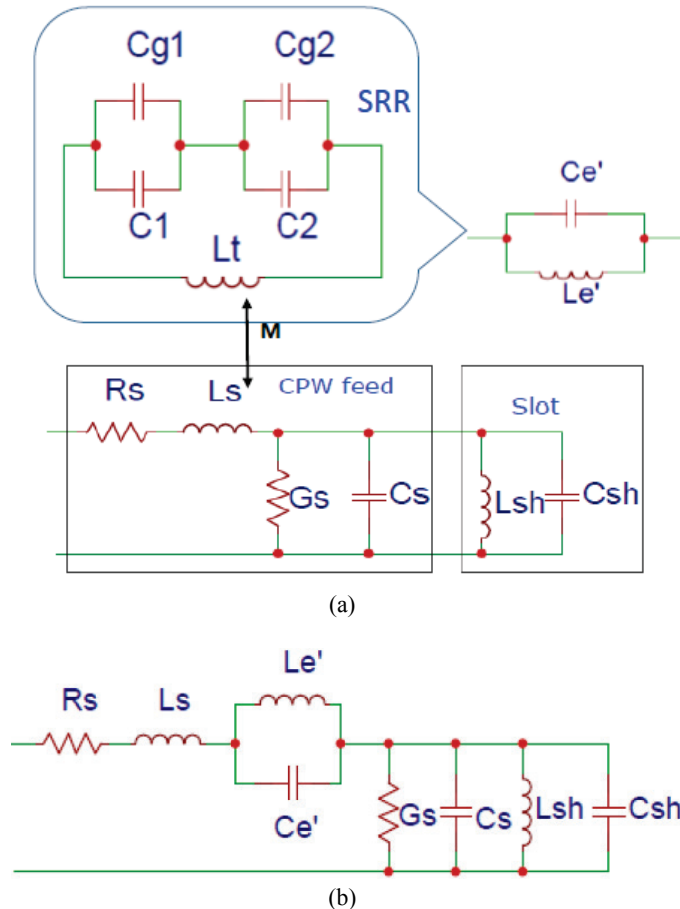


Fig. 3. Equivalent circuit modeling of SRR and proposed antenna:
 (a) SRR loaded slot with CPW feed,
 (b) simplified equivalent circuit of proposed antenna

In the proposed antenna, the wideband CP is achieved by combining slot and SRR resonance. The truncated square slot antenna provides lower band resonance, Eq. (1) is used to calculate the slot resonance frequency. The rotated SRR gives the higher band resonance which is calculated from Eq. (2). Both resonances are independently tuned to optimize the wideband CP performance. Fig. 4 shows the simulated reflection coefficient magnitude and axial ratio for different design stages of the proposed antenna. The CPW fed conventional square slot (case a) antenna gives resonance at 2.78 GHz with better impedance matching. However, the axial ratio plot in Fig. 2(b) shows it generates linear polarization. The corner truncated square slot resonates (case b) at 4.12 GHz with wide impedance bandwidth with the good axial ratio. The truncated square slot gives axial ratio bandwidth of 17.69% at lower band. To improve the axial ratio bandwidth, the SRR with inner ring rotated 90° is etched on the top of the substrate within the slot antenna. When SRR is excited by the axial magnetic field of the slot antenna, it acts as a magnetic loop and radiates independently without affecting slot resonance. The split gaps in the conventional SRR are aligned diametrically in the same axis. When split gaps of SRR rings are aligned 90° with each other, they exhibit orthogonal electric fields between two split gaps of the rings produces circular polarization. By optimizing split gaps of two rings better axial ratio is achieved. The rotated SRR

loaded truncated slot antenna (case c) gives upper SRR band at 4.62 GHz without affecting the slot resonance. The truncated square slot with rotated SRR enhances the axial ratio bandwidth to 21.81%. The resonances of truncated slot and SRR are tuned independently to optimized axial ratio bandwidth.

The variation in the electric field at different time instances t=0, T/4 is shown in Fig. 5(a) and (b), it shows that LHCP wave is radiated in the +z direction. The electric field distribution of SRR at 4.62 GHz is shown in Fig. 5(c). It is observed that the electric fields are orthogonal to each other in the two split gaps of inner and outer rings, which produces CP wave at SRR resonance. The feed-line is shifted from the center to match the impedance and efficiently couple the SRR. The variation in impedance and axial ratio curves is shown in Fig. 6(a) and (b). The good impedance matching and axial ratio are obtained with $f_0=3$ mm. The impedance bandwidth and axial ratio of the antenna with and without SRR are shown in Fig. 6(c) and (d). There is no significant variation in the impedance bandwidth, but the axial ratio bandwidth is improved significantly after introducing SRR. The split gap variation of SRR is shown in Fig. 7. In the figure it is observed that the S_{11} and AR are significantly varied in SRR resonance. So the optimized value is given to achieve best performance.

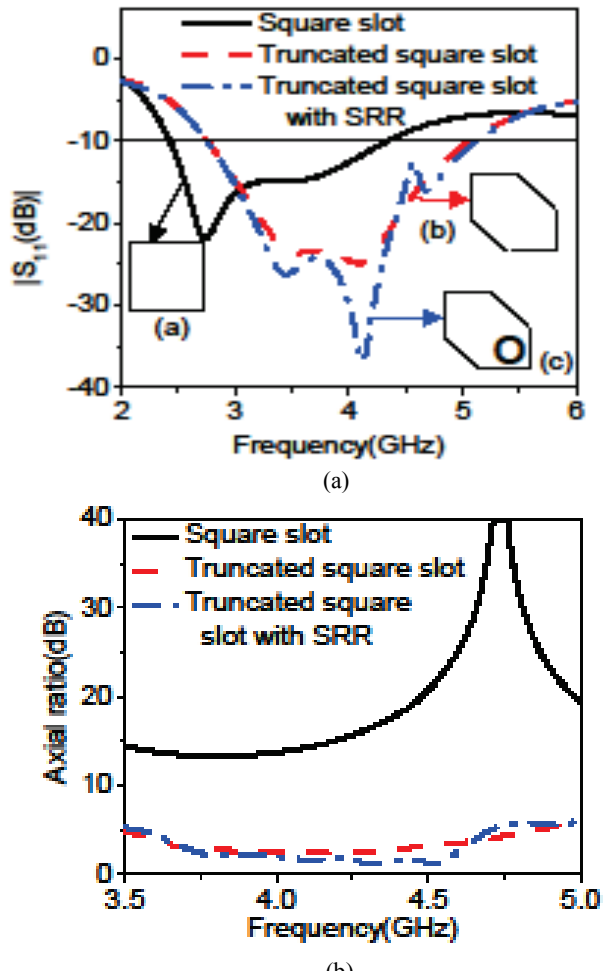


Fig. 4. Simulated reflection coefficient and axial ratio of different stages of planar slot antenna: (a) S_{11} and (b) axial ratio

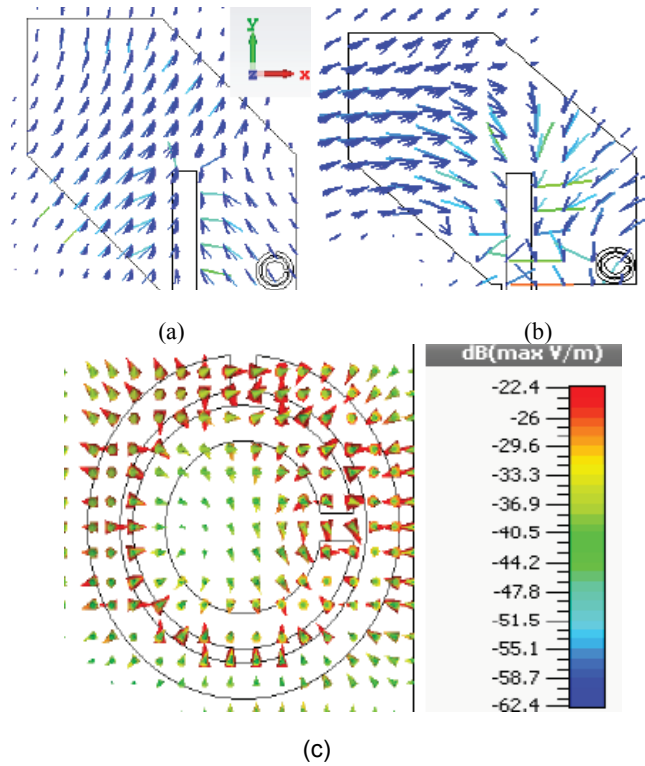


Fig. 5. Simulated electric field distribution at different time instances at slot resonance 4.12 GHz: (a) $t=0$, (b) $t=T/4$, and (c) electric field distribution at SRR resonance 4.6 GHz

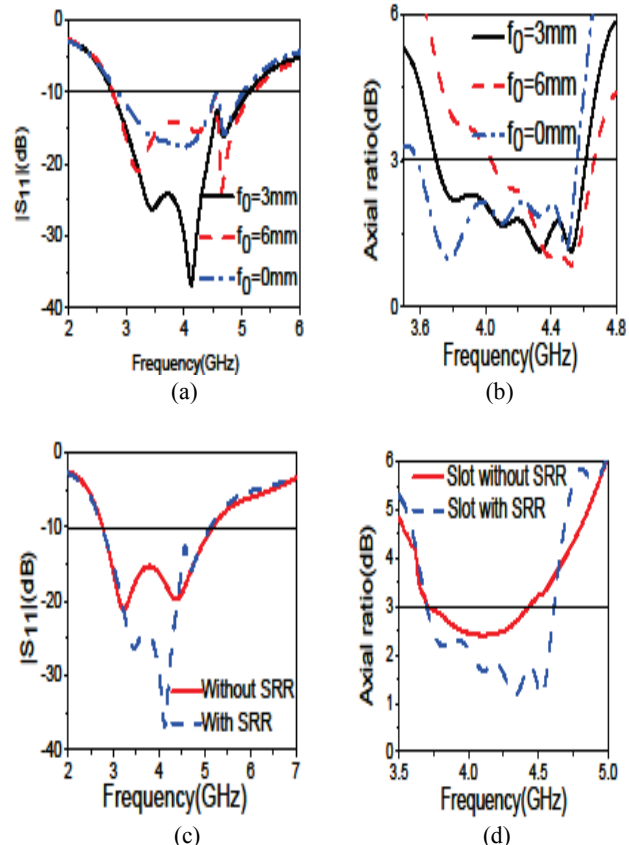


Fig. 6. Simulated reflection coefficient and axial ratio of antenna: (a) S_{11} with feed shift, (b) axial ratio with feed shift, (c) S_{11} with and without SRR, and (d) axial ratio with and without SRR

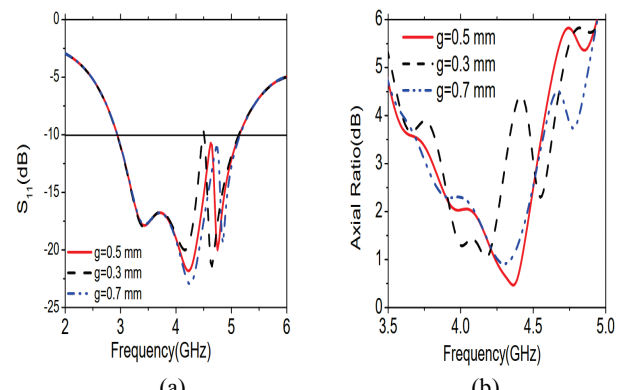


Fig. 7. Simulated reflection coefficient and axial ratio of antenna for split gap variation in SRR: (a) S_{11} and (b) axial ratio

IV. EXPERIMENTAL RESULTS

The fabricated prototype of the proposed antenna is shown in Fig. 8(a). The simulated impedance bandwidth ($|S_{11}| < -10 \text{ dB}$) of 56.36% from 2.77 GHz to 5.10 GHz and measured impedance bandwidth of 61.40% from 2.57 GHz to 5.10 GHz is achieved. The simulated axial ratio bandwidth of 21.81% from 3.7 GHz to 4.6 GHz and measured axial ratio bandwidth of 21.68% from 4 GHz to 4.9 is achieved. The comparison between simulated and measured results of the reflection coefficient, axial ratio and gain is shown in Fig. 8(b), (c) and (d). There is a 1 dB variation over the axial ratio bandwidth with a measured peak gain of 2.74 dB at 4.12 GHz. The axial ratio is obtained at a tilt angle of 20° from broadside, which is due to the truncation effect of the slot antenna. The radiation pattern of the proposed antenna both in xz and yz plane at frequencies 3.8 GHz, 4.12 GHz and 4.8 GHz are shown in Fig. 9. The RHCP polarization level of -17dB is achieved with respect to LHCP at a beam tilting angle of 20°. The measured results are in good agreement with simulated results with little variation because of the fabrication error and connector losses which are not considered during simulation. The performance comparison of proposed work is given in Table 1.

TABLE1
THE PERFORMANCE COMPARISON OF PROPOSED DESIGN
WITH OTHER WORKS

Ref.	IBW (%)	ARBW (%)	Gain (dB)
[7]	25.9	16.9%	2.3
[18]	36.3	20.4	11.1
[19]	23	18.3	10
Proposed work	61.4	21.69	2.7

*IBW: Impedance Bandwidth
ARBW: Axial Ratio Bandwidth

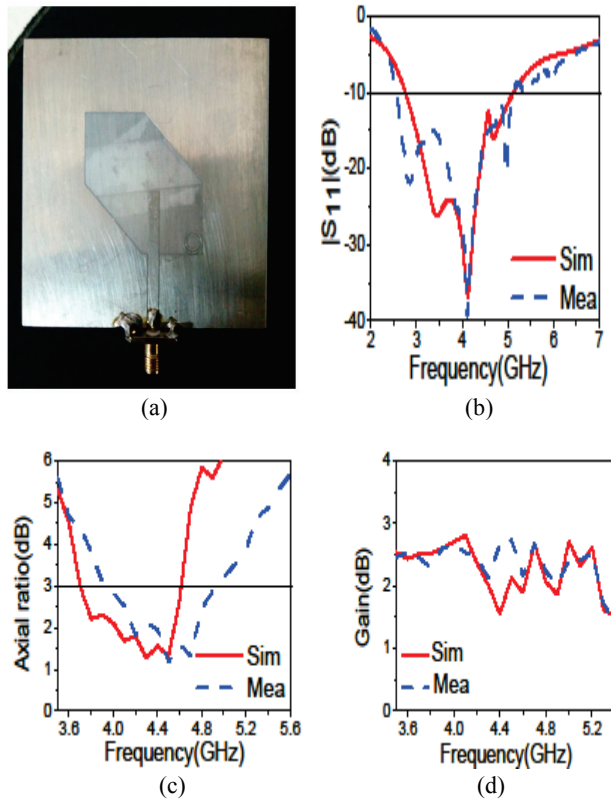


Fig. 8. (a) Fabricated prototype of the proposed antenna, (b) simulated and measured reflection coefficient, (c) simulated and measured axial ratio, and (d) simulated and measured gain

V. SOIL SENSING

The proposed wideband CP antenna is designed on the top side of the substrate and back side of the antenna is directly placed on the soil to be tested. The antenna can be shielded with a plastic sheet to avoid short circuit with the water content of the soil. Since the air gap between soil and antenna change the reflection coefficient slightly, the air gap between the soil and the antenna is also considered in the simulation. Two types of soil model are simulated based on the change in permittivity of the soil. Dry soil has a permittivity of 2.4 and wet soil has a permittivity of 13.8 [16]. When the antenna is placed on the soil, the effective permittivity of the antenna is changed and its reflection coefficient varies as shown in Fig. 10(a). The antenna with dry soil has no significant change in the reflection coefficient because its permittivity is near to the permittivity of substrate used to design antenna. Since wet soil has a high value of permittivity, there is a significant change in reflection coefficient and it is measured using a vector network analyzer (VNA). The comparison between the simulated and measured reflection coefficient magnitude of dry and wet soil is shown in Fig. 10(b). It is observed that the wet soil has higher permittivity and resonance is shifting towards lower frequency compared to dry soil. Based on the variation in reflection coefficient between dry and wet soil, we can also estimate the soil moisture content present in the soil. The simulated results are in good agreement with measured results.

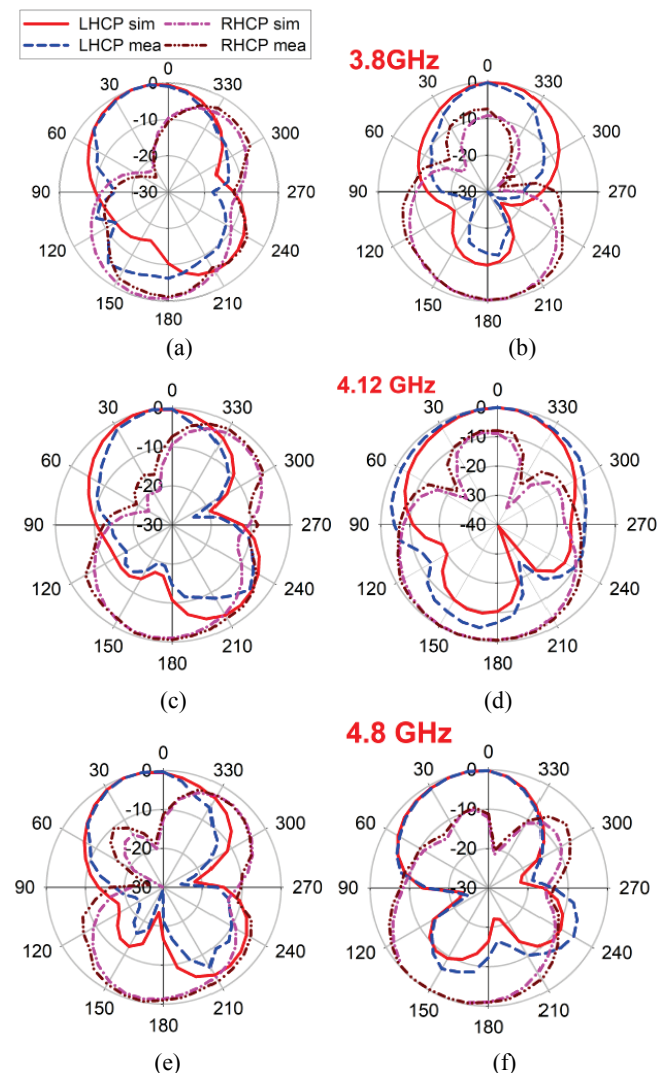


Fig. 9. Comparison between simulated and measured radiation pattern at different CP frequencies: (a) xz plane, (b) yz plane, (c) xz plane, (d) yz plane, (e) xz plane, and (f) yz plane

VI. CONCLUSION

A CPW fed single layer wideband circularly polarized truncated square slot antenna loaded with rotated SRR is presented. The wideband performance is obtained by combining slot and SRR mode resonances. The bands are tuned independently to achieve optimized wide axial ratio bandwidth. The measured impedance bandwidth of 2.53 GHz and 3-dB axial ratio bandwidth of 0.9 GHz is achieved. The proposed antenna is useful for soil moisture sensing, military, radar and microwave sensing application where CP is essential.

REFERENCES

- [1] S. S. Gao, Q. Luo and F. Zhu, *Circularly Polarized Antennas*, John Wiley Sons Ltd, 2014.
- [2] R. Cao and S. C. Yu, "Wideband Compact CPW-fed Circularly Polarized Antenna for Universal UHF RFID Reader", *IEEE Transactions on Antennas and Propagation*, vol. 63, no. 9, pp. 4148-4151, September 2015.

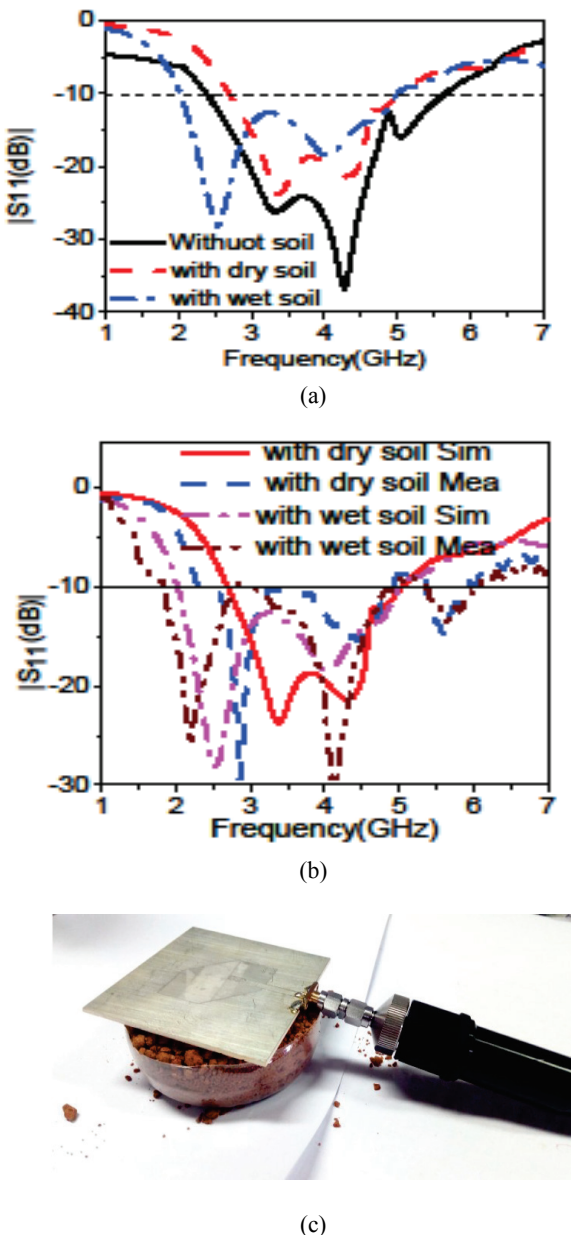


Fig. 10. (a) Simulated reflection coefficient of wideband CP antenna with and without soil, (b) comparison between simulated and measured reflection coefficient of wideband CP antenna with dry and wet soil, and (c) testing environment

- [3] J. Y. Sze, J. C. Wang and C. C. Chang, "Axial-Ratio Bandwidth Enhancement of Asymmetric-CPW-fed Circularly-Polarised Square Slot Antenna", *Electronics Letters*, vol. 44, no. 18, pp. 1048-1049, August 28 2008.
- [4] R. K. Saini, S. Dwari and M. K. Mandal, "CPW-fed Dual-band Dual-sense Circularly Polarized Monopole Antenna", *IEEE Antennas and Wireless Propagation Letters*, vol. 16, pp. 2497-2500, 2017.
- [5] R. Xu, J. Li, Y. X. Qi, Y. Guangwei and J. J. Yang, "A Design of Triple-Wideband Triple-Sense Circularly Polarized Square Slot Antenna", *IEEE Antennas and Wireless Propagation Letters*, vol. 16, pp. 1763-1766, 2017.

- [6] R. K. Saini and S. Dwari, "A Broadband Dual Circularly Polarized Square Slot Antenna", *IEEE Transactions on Antennas and Propagation*, vol. 64, no. 1, pp. 290-294, January 2016.
- [7] L. Ge, C. Y. D. Sim, H. L. Su, J. Y. Lu and C. Ku, "Single-layer Dual-Broadband Circularly Polarised Annular-slot Antenna for WLAN Applications", *IET Microwaves, Antennas Propagation*, vol. 12, no. 1, pp. 99-107, 2018.
- [8] H. Liu, Y. Liu and S. Gong, "Broadband Microstrip-CPW fed Circularly Polarised Slot Antenna with Inverted Configuration for L-band Applications", *IET Microwaves, Antennas Propagation*, vol. 11, no. 6, pp. 880-885, 2017.
- [9] A. Abed, M. Singh and A. Jawad, "Investigation of Circular Polarization Technique in Q-slot Antenna", *International Journal of Microwave and Wireless Technologies*, vol. 12, no. 2, pp. 176-182, 2020, doi: 10.1017/S1759078719001107
- [10] Y. H. Ren, J. Ding, C. J. Guo, Y. Qu and Y. C. Song, "A Wideband Dual-Polarized Printed Antenna Based on Complementary Split-Ring Resonators", *IEEE Antennas and Wireless Propagation Letters*, vol. 14, pp. 410-413, 2015.
- [11] D. Sarkar, K. Saurav and K. V. Srivastava, "Multi-band Microstrip-fed Slot Antenna Loaded with Split-ring Resonator", *Electronics Letters*, vol. 50, no. 21, pp. 1498-1500, October 9 2014.
- [12] V. Sharma, N. Lakwar, N. Kumar and T. Garg, "Multiband Low-cost Fractal Antenna based on Parasitic Split Ring Resonators", *IET Microwaves, Antennas and Propagation*, vol. 12, no. 6, pp. 913-919, 2018.
- [13] K. Kandasamy, B. Majumder, J. Mukherjee and K. P. Ray, "Dual-Band Circularly Polarized Split Ring Resonators Loaded Square Slot Antenna", *IEEE Transactionson Antennas and Propagation*, vol. 64, no. 8, pp. 3640-3645, August 2016.
- [14] A. Cataldo, G. Monti, E. De Benedetto, G. Cannazza and L. Tarricone, "A Noninvasive Resonance-Based Method for Moisture Content Evaluation Through Microstrip Antennas", *IEEE Transactions on Instrumentation and Measurement*, vol. 58, no. 5, pp. 1420-1426, May 2009.
- [15] P. Soontornpipit, C. M. Furse, Y. C. Chung and B. M. Lin, "Optimization of a Buried Microstrip Antenna for Simultaneous Communication and Sensing of Soil Moisture", *IEEE Transactions on Antennas and Propagation*, vol. 54, no. 3, pp. 797-800, March 2006.
- [16] T. Toba and A. Kitagawa, "Wireless Moisture Sensor using a MicrostripAntenna", *Journal of Sensors*, vol. 2011, Article ID 827969, 6 pages, 2011.
- [17] S. K.K. Dash, T. Khan and B. K. Kanaujia, "Circularly Polarized Dual Facet SpiralFed Compact Triangular Dielectric Resonator Antenna for Sensing Applications", *IEEE Sensors Letters*, vol. 2, no. 1, pp. 1-4, March 2018.
- [18] M. Sun, N. Liu, L. Zhu and G. Fu, "Wideband Circularly Polarized Sequentially Rotated Microstrip Antenna Array with Sequential-Phase Feeding Network", *Journal of Communications and Information Networks*, vol. 5, no. 3, pp. 350-357, September 2020, doi: 10.23919/JCIN.2020.9200898
- [19] L. Wang and Y. -F. En, "A Wideband Circularly Polarized Microstrip Antenna with Multiple Modes", *IEEE Open Journal of Antennas and Propagation*, vol. 1, pp. 413-418, 2020, doi: 10.1109/OJAP.2020.3009884
- [20] C. Saha and J. Y. Siddiqui, "Theoretical Model for Estimation of Resonance Frequency of Rotational Circular Split-Ring Resonators", *Electromagnetics*, vol. 32, pp. 345-355, 2012.
- [21] P. Sharma and K. Gupta, "Analysis and Optimized Design of Single Feed Circularly Polarized Microstrip Antennas", *IEEE Transactions on Antennas and Propagation*, vol. 31, no. 6, pp. 949-955, November 1983.